Absence of dynamical steps in the exact correlation potential in the linear response regime

Kai Luo,[1] Peter Elliott,[2] and Neepa T. Maitra[1]

[1]*Department of Physics and Astronomy, Hunter College and the Graduate Center of the City University of New York, 695 Park Avenue, New York, New York 10065, USA*

[2]*Max-Planck-Institut für Mikrostrukturphysik, Weinberg 2, 06120 Halle (Saale), Germany*

(Received 24 May 2013; published 17 October 2013)

Recent work [Phys. Rev. Lett. **109**, 266404 (2012)] showed that the exact exchange-correlation potential of time-dependent density-functional theory generically displays dynamical step structures. These have a spatially nonlocal and time-nonlocal dependence on the density in real-time dynamics. The steps are missing in the usual approximations, which consequently yield inaccurate dynamics. Yet these same approximations often yield good linear response spectra. Here we investigate whether the steps appear in the linear response regime, when the response is calculated from a real-time dynamics simulation, by examining the exact correlation potential of model two-electron systems at various times. We find there are no step structures in regions where the system response is linear. Step structures appear in the correlation potential only in regions of space where the density response is nonlinear; these regions, having exponentially small density, do not contribute to the observables measured in linear response.

DOI: 10.1103/PhysRevA.88.042508 PACS number(s): 31.15.ee, 71.15.Qe, 71.15.Mb

I. INTRODUCTION

Time-dependent density functional theory (TDDFT) is now a method of choice for the calculation of excitation spectra and response properties in materials science and quantum chemistry [1–3]. It maps the system of interacting electrons into a fictitious one of noninteracting fermions, called the Kohn-Sham (KS) system, from which all properties of the original system may be exactly extracted in principle. Therefore large systems of relevance in biochemistry and nanoscience may be treated. The KS fermions evolve in a one-body potential, $v_s(\mathbf{r},t)$, which has the property that the exact one-body density of the system of interacting electrons is exactly reproduced by the noninteracting KS fermions. However, an essential component of this potential, the exchange-correlation (xc) potential, is unknown and must be approximated as a functional of the density, the interacting initial state Ψ_0, and the noninteracting initial state Φ_0: $v_{\rm xc}[n,\Psi_0,\Phi_0](\mathbf{r},t)$. The vast majority of applications today use an adiabatic approximation, meaning one where the instantaneous density is input into a ground-state xc approximation: $v^A_{\rm xc}[n,\Psi_0,\Phi_0](\mathbf{r},t) = v^{\rm g.s.}_{\rm xc}[n(\mathbf{r},t)]$. All memory dependence is neglected. The adiabatic approximation is behind the linear response results whose success has propelled TDDFT forward, and it is implicitly assumed in all the readily available codes today. Cases for which the adiabatic approximation fail are known (e.g., states of double-excitation character, long-range charge-transfer excitations between open-shell fragments, conical intersections), and users are generally aware to apply caution when interpreting the TDDFT results in these cases. Still, TDDFT has proven itself remarkably useful in its balance between accuracy and efficiency for spectra and response, and functional developments are ongoing [2–4].

TDDFT is not limited to the linear response regime. Indeed, given the dearth of alternative practical methods of solving correlated electron dynamics in nonequilibrium situations, the nonlinear regime is arguably more important for TDDFT. Moreover, due to the recent intense progress in attosecond technology, the control and study of electron dynamics, with the concomitant control and study of nuclear dynamics, are becoming an experimental reality. However, for real-time nonequilibrium dynamics, much less is known about the accuracy of the usual functionals in TDDFT, and from comparisons with the few available exactly solvable systems, it appears that memory effects, missing in the usual adiabatic approximations, can be significant. In this context, hydrodynamic-inspired approaches (e.g., Refs. [5–7]), and orbital-dependent functionals [8], among others, are being explored.

Recent work has shown the prevalence of dynamical step structures in the time-dependent xc potential in far-from-equilibrium situations [9–11]. These step structures were found to arise in a variety of dynamics, from resonant Rabi oscillations in a model atom and molecule [10,11], to dynamics under an arbitrary strong field [10], to quasiparticle propagation in a semiconducting wire [9]. The steps were found to have a nonlocal dependence on the density in both space and time; it was shown that even an adiabatically exact approximation fails to capture them. Typical approximations in use today do not contain these structures, resulting in inaccurate dynamics, as shown in the examples in Refs. [10,11]. Yet these same approximations do give good spectra for these systems. The question then arises: what happens to these steps in the linear response regime? In this paper, we show that the steps are in fact a *nonlinear* response phenomenon and do not appear when the response of the system is linear. To show this, we calculate the time-dependent correlation potential in model two-electron systems under several linear response situations, including a weak field smoothly turned on and off, as well as evolution under a δ kick. A nonadiabatic kernel has been shown to be essential to obtain excitations of double-excitation character [12,13], but we show here that the nonadiabatic step of Ref. [10] is an unrelated phenomenon.

The rest of the paper is organized as follows: In Sec. II, we first introduce the model systems used in our study. We then proceed to find the time-dependent correlation potential in linear response to a smoothly-turned-on weak field (Sec. II A) and to a δ kick (Sec. II B). In Sec. III we find explicit

expressions for the terms in the correlation potential that scale linearly with the system's response and, finally, Sec. IV contains our conclusions.

II. DYNAMICS IN THE LINEAR RESPONSE REGIME

The system we will mostly focus on in this paper is a one-dimensional (1D) model of the He atom; the Hamiltonian can be written as

$$\hat{H} = \hat{H}_0 + \hat{H}_1(t) = \hat{T} + \hat{V}(t) + \hat{W}, \tag{1}$$

where $\hat{T} = \sum_i -\frac{1}{2}\frac{\partial^2}{\partial x_i^2}$ is the kinetic energy, $\hat{V}(t) = \sum_i[-2/(x_i^2+1)^{1/2} - x_i\mathcal{E}(t)]$ is the external potential, and $\hat{W} = 1/[(x_1-x_2)^2+1]^{1/2}$ is the soft-Coulomb electron-electron interaction [14]. The sums go over two fermions. (Atomic units $e^2 = \hbar = m_e = 1$ are used throughout the paper.) This soft-Coulomb model is commonly used in analyzing functionals, since it is numerically straightforward to find the exact time-evolving wave function, and then extract the exact exchange and correlation potentials for comparison with approximations [15–23]. We will apply weak off-resonant fields, represented by $\mathcal{E}(t)$ above, to stimulate linear response of the system, as will be detailed below.

Since all double excitations in the He atom lie in the continuum, we instead consider a model of a quantum dot to study this issue, taking $\hat{V}(t) = \sum_i[\frac{1}{2}x_i^2 + x_i^2\mathcal{F}(t)]$. The time-dependent driving in this case is modified from the usual dipole form to a quadratic form, since the linear dipole perturbation only couples to the first-excited state which is predominantly a single excitation [24,25].

For two electrons in a spin-singlet, choosing the initial KS state as a doubly occupied spatial orbital $\phi(\mathbf{r},t)$ means that the exact KS potential for a given density evolution can be found easily (see, e.g., Refs. [10,26]). In 1D, we have

$$v_{\rm S}(x,t) = -\frac{[\partial_x n(x,t)]^2}{8n^2(x,t)} + \frac{\partial_x^2 n(x,t)}{4n(x,t)} - \frac{u^2(x,t)}{2} - \int^x \frac{\partial u(x',t)}{\partial t}dx', \tag{2}$$

where $u(x,t) = j(x,t)/n(x,t)$ is the local "velocity," $n(x,t)$ is the one-body density, and $j(x,t)$ is the current density. We numerically solve the exact time-dependent two-electron wave function, obtain the one-body density and current density, and insert them into Eq. (2). The exchange-potential in this case is simply minus half the Hartree potential, $v_{\rm X}(x,t) = -v_{\rm H}(x,t)/2$, with $v_{\rm H}(x,t) = \int w(x',x)n(x',t)dx'$, in terms of the two-particle interaction $w(x',x)$. Therefore, we can directly extract the correlation potential using

$$v_{\rm C}(x,t) = v_{\rm S}(x,t) - v_{\rm ext}(x,t) - v_{\rm H}(x,t)/2, \tag{3}$$

where $v_{\rm ext}(x,t)$ is the external potential applied to the system.

Computational details. We use OCTOPUS [27,28] to compute the exact wave function. The time-dependent Schrödinger equation is solved by first mapping the Hamiltonian of two interacting electrons in 1D onto the Hamiltonian of one electron in two dimensions (2D). We use a grid of size 40.00 a.u. and grid spacing of 0.1 a.u. The approximated enforced time-reversal symmetry method was used in the propagation, with a time step of 0.001 a.u. The densities and current densities are then extracted and a standard finite-difference scheme is used get the time derivative of the velocity.

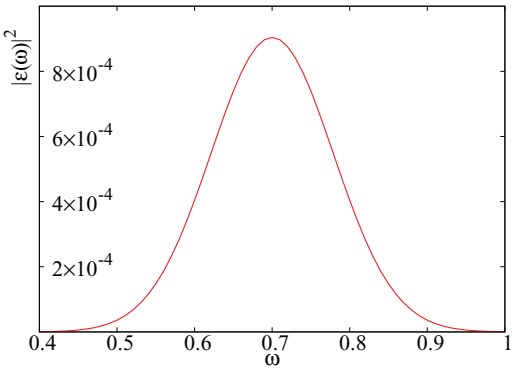

FIG. 1. (Color online) This plot shows the modulus square of the Fourier-transformed field of strength of $\epsilon_1 = 0.0067$ a.u., which includes the first several excitation energies.

A. Dynamics in a Gaussian-shaped pulse

The examples in Ref. [10] began in the ground state and either applied a weak resonant field or a strong arbitrary field to the system, or began in a superposition of a ground and excited state. None of these situations are the territory of linear response. Instead here, we apply a weak off-resonant field, but with an envelope such that a number of excitations fall under it. To this end, we apply a weak electric field $\mathcal{E}(t)$ with the following Gaussian envelope:

$$\mathcal{E}(t) = \epsilon_\alpha e^{-[\frac{t-3T_0}{\sqrt{2}T_0}]^2}\cos(\Omega_0 t), \tag{4}$$

where $T_0 = 2\pi/\Omega_0$ is the period corresponding to the central frequency, and ϵ_α is the peak field strength (see below). Figure 1 shows the power spectrum for strength ϵ_1; excitations of the 1D He model of frequency 0.533, 0.672, 0.7125, ... a.u. lie in its bandwidth. Here we have chosen $\Omega_0 = 0.7$ a.u., but our conclusions are independent of this value.

We choose a weak-field strength $\epsilon_1 = 0.0067$ a.u. such that the predominant response of the system is linear. We then apply weaker fields ϵ_α of strengths $\epsilon_{0.50} = \frac{\epsilon_1}{2}$ and $\epsilon_{0.25} = \frac{\epsilon_1}{4}$.

The top-left panel of Fig. 2 shows that the density response, defined as $\delta n_\alpha(x,t) = n_\alpha(x,t) - n(x,0)$, predominantly scales linearly with the field strength: plots of $\delta n_\alpha/\alpha$ lie essentially on top of each other. The correlation potential response, in the lower left panel, in region $\approx(-5,5)$ also scales linearly with the applied field but deviates from linearity outside this region, displaying step and peak structures; these are also evident in the full correlation potential plotted in the top-right panel. Zooming into the tail regions of the densities (see, e.g., inset of top panel), we see in fact that the density response is not linear in these regions. The steps and peaks in the nonlinear region do not scale with the field strength; we do not expect them to because the response is not linear, and they also do not have any higher-order consistent scaling behavior with the field strength.

We have checked that the step features are not numerical artifacts: they are converged with respect to the size of the box and grid spacing. Changing these parameters may change the details of the noise in the small oscillations visible in $\delta v_{\rm C}$

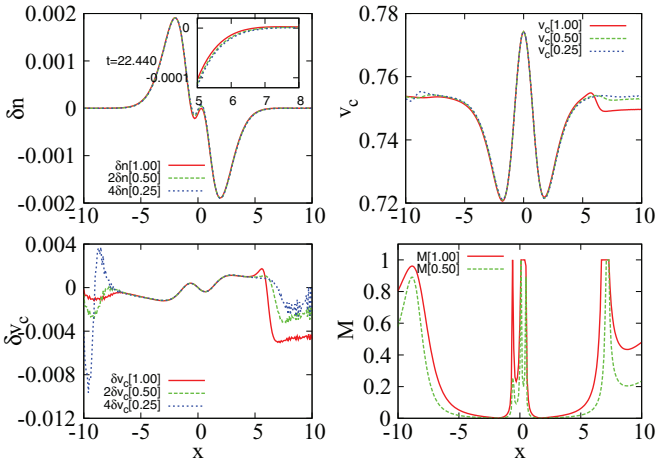

FIG. 2. (Color online) Densities and correlation potentials at time $t = 22.440$ a.u. The top-left shows the scaled density response $\delta n_\alpha(x,t)/\alpha$ for the three values of α indicated. The inset zooms in on the scaled density response in the outer region. The top-right shows the correlation potentials at different field strengths. The bottom-left panel plots the scaled correlation potential response, $\delta v_{c,\alpha}(x,t)/\alpha$. The steps of the correlation potentials occur where the density response is nonlinear. The lower-right panel plots the deviation from linearity, M_α, of Eq. (5).

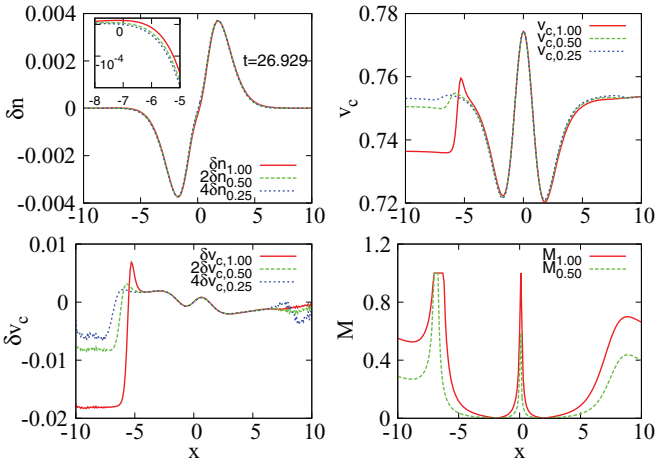

FIG. 3. (Color online) Densities and correlation potentials at time $t = 26.929$ a.u. See caption of Fig. 2 for details.

(much smaller scale than the scale of the step itself) but do not change the overall structure. This is true for all the graphs shown in the paper.

To quantify the deviation from linearity we next define a measure, which we plot in the lower-right panel. Since the weakest strength is closest to the ideal linear response limit, we define the deviation relative to this strength and define:

$$M_\alpha = \frac{|\delta n_\alpha - 4\alpha\delta n_{0.25}|}{|\delta n_\alpha| + 4\alpha|\delta n_{0.25}|}. \tag{5}$$

If the density response at field strength α was truly linear, the numerator would vanish (within the approximation that when $\alpha = 0.25$ the system response is linear); and it is trivially zero when $\alpha = 0.25$. The measure takes values from 0 to 1, growing as the degree of nonlinearity grows. Note that when the signs of δn_α and $\delta n_{0.25}$ are opposite, the measure takes the value of 1. In the lower-right panel in Fig. 2, we see that, aside from a sharp peak structure near $x = 0$, M_α is small in the region $x \approx (-5,5)$, then grows outside this region, peaking and remaining large after the peak. The sharp structure near $x = 0$ occurs due to the density responses themselves going through zero near the origin. The step structures in the correlation potential appear only in the outer region, where the measure is appreciable, i.e., the density response is significantly nonlinear.

Figures 3 and 4 show the density responses and correlation potentials plotted in the same way, at two other times, $t = 26.929$ a.u. and $t = 31.417$ a.u. The same conclusions can be drawn as for the earlier time, and in fact for all the different times throughout the time propagation that we analyzed: *step structures appear only in regions where the system's response is nonlinear*. We did not find a single time at which steps occurred in a region where the density response is linear. The step structures do not scale in any consistent way with the field strength. (Where the system response is linear, the correlation potential response scales linearly with the field, as expected.) There are times at which the step is abnormally large: this tends to happen in close-to-nodal structures of the density and is likely a feature only of two-electron systems.

We note that regions of nonlinear system response are typical in linear response calculations: essentially, the term representing the field in the Hamiltonian $H_0 + \mathcal{E}(t)x$ gets larger than the field-free term for large x, so a perturbative treatment of it in that region is no longer valid. However, such a calculation is still considered to be in the linear response regime, since these regions contribute negligibly to practical observables extracted from the system dynamics.

B. Dynamics under a "δ kick"

A common way to obtain linear response spectra from real-time dynamics is to apply a "δ kick" to the system at the initial time and measure the subsequent free evolution [29]. That is, $\mathcal{E}(t) = k\delta(t)$, so that we can write $\Psi(t = 0^+) = e^{ik\hat{x}}\Psi(t = 0)$. For sufficiently small kick strengths k, the system response is linear in k. Fourier transforming the time-dependent dipole moment yields the spectrum shown in Fig. 5, where a value

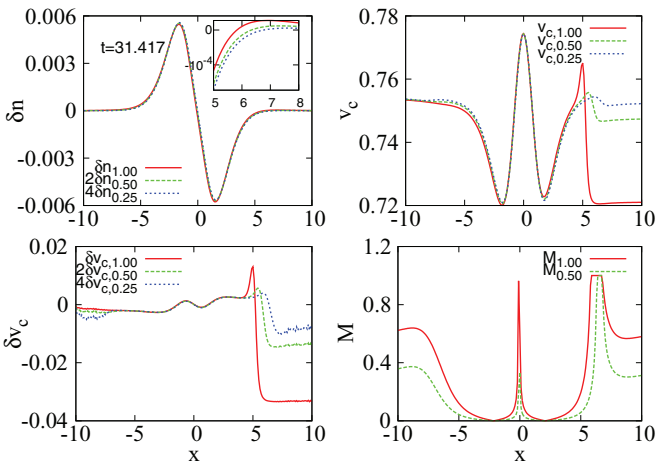

FIG. 4. (Color online) Densities and correlation potentials at time $t = 31.417$ a.u. See caption of Fig. 2 for details.

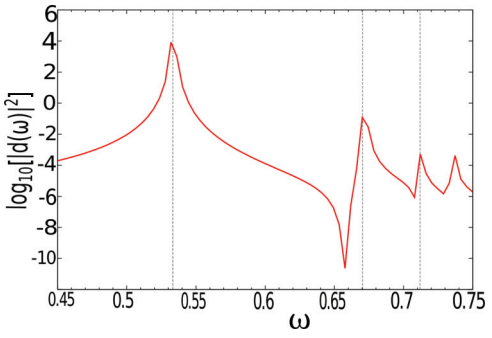

FIG. 5. (Color online) The dipole power spectrum obtained from solving the time-dependent Schrödinger equation. Vertical dashed lines indicate the dipole-allowed singlet transition energies, which agree with the energy spectrum. (Note that the relative oscillator strengths are not accurate because the propagation time was not long enough.)

of $k = 0.01$ was used. The peaks correspond to the singlet excited states of odd parity as these are dipole allowed. The peak frequencies shown can be confidently assigned to these states only up to about $\omega \sim 0.73$ a.u., because the excited states of energies higher than this have spatial extent too large for the size of the box in our calculation (we have checked convergence with respect to box size for the lower excitations).

Now we consider the same analysis as in the previous case: we halve k and study the response of the correlation potential and density, looking for the step feature. The main difference from the Gaussian-pulse field is that now all the dipole-allowed singlet excited states are equally stimulated: the power spectrum for the δ kick is uniform.

Figures 6 and 7 show the response densities and correlation potentials at two snapshots of time: 400 and 1400 a.u., respectively. Similar graphs appear at the other times we looked at. We again see steps and (sometimes large and oscillatory) peak-like structures but, again, they appear only in the region of nonlinear density response; regions that contribute negligibly to the linear response observables. Once again, these structures are fully nonlinear, in that there is no consistent scaling of their size with the field strength.

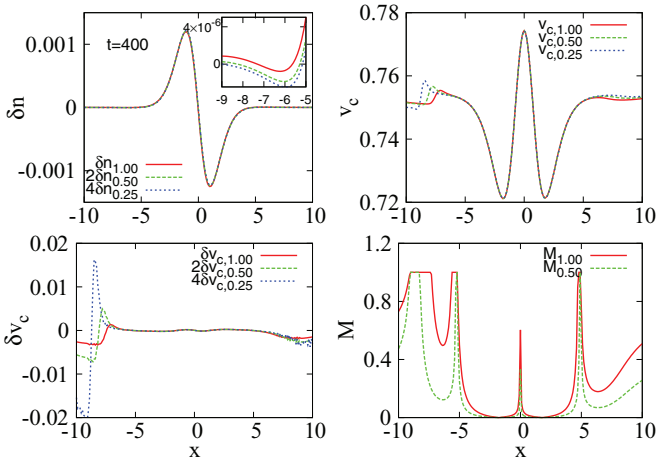

FIG. 6. (Color online) At time 400 a.u. after the kick is applied, the response densities and correlation potentials are shown; please refer to Fig. 1 for the details of the panels.

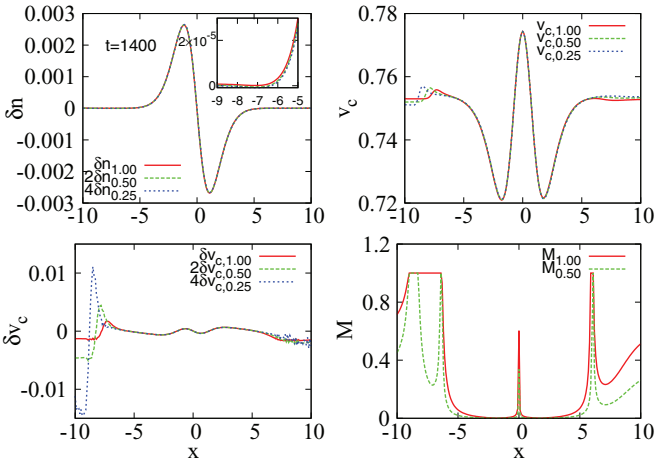

FIG. 7. (Color online) As in Fig. 6 but for time 1400 a.u.

III. LINEAR TERMS IN v_c IN FIELD-FREE EVOLUTION OF PERTURBED GROUND STATE

The dynamical step that was found in typical nonlinear dynamics situations arises from the fourth term of Eq. (2), as discussed in Ref. [10]. Here we analyze that term, as well as the full correlation potential, in a linear response situation by explicitly finding the terms that scale linearly with the deviation from the ground state.

We consider field-free evolution of a perturbed ground state; for example, as would occur in the δ-kicked propagation of the previous section. We can then expand the wave function at time t in terms of the eigenstates Ψ_m of the unperturbed system, as

$$\Psi(t) = e^{-iE_0t}\left(\Psi_0 + \sum_m c_m e^{-i\omega_m t}\Psi_m\right), \tag{6}$$

where Ψ_0 is the ground state, $\omega_m = E_m - E_0$ are excitation frequencies, and c_m are expansion coefficients, to be considered the small parameter. For example, in the δ-kick of the previous section, $c_m = ik\langle\Psi_0|\hat{x}|\Psi_m\rangle$ (where, for the two-electron case, $\hat{x} = x_1 + x_2$). (Note that in the general case, c_0 need not be zero.) Then we may write, to first order in c_m,

$$n(x,t) = n_0(x) - 2i\sum_m c_m \sin(\omega_m t) n_{0m}(x), \tag{7}$$

where $n_0(x)$ is the ground-state density and $n_{0m}(x) = 2\int dx'\Psi_0(x,x')\Psi_m(x,x')$ is the mth transition density. Also, we have to linear order in c_m,

$$j(x,t) = i\sum_m c_m \cos(\omega_m t) j_{0m}, \tag{8}$$

where $j_{0m}(x) = 2\int dx'[\Psi_m\partial\Psi_0/\partial x - \Psi_0\partial\Psi_m/\partial x]$. So, to linear order in c_m,

$$\int^x \partial_t u(x',t)dx' = -i\sum_{m\neq 0} c_m\omega_m \sin(\omega_m t)\int^x \frac{j_{0m}(x')}{n_0(x')}dx'. \tag{9}$$

If there is any step in the correlation potential that appears at linear order, it must appear in this term. From computing just the excited-state wave functions and their energies, the right-hand side can easily be computed. Further, expanding all

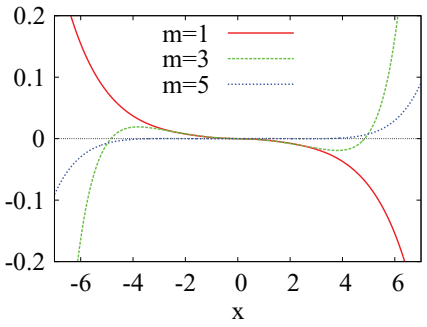

FIG. 8. (Color online) Correlation responses for the δ-kicked soft-Coulomb well, from the first three terms of Eq. (10).

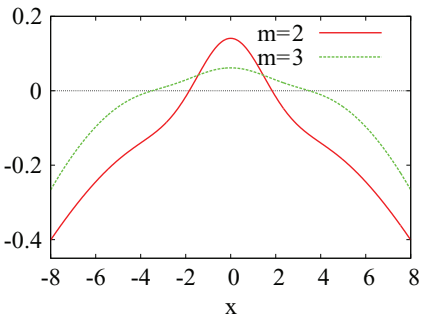

FIG. 9. (Color online) Correlation-potential responses from double-excitation contributions in the quadratically kicked harmonic potential.

terms in Eq. (2) to linear order and using Eq. (3), we get the response of the correlation potential to first order:

$$\delta v_{\rm C} = \sum_{m\neq 0} i c_m \sin(\omega_m t)\left[\frac{(\partial_x n_0)^2}{2n_0^2}\left(\frac{\partial_x n_{0m}}{\partial_x n_0} - \frac{n_{0m}}{n_0}\right) - \frac{\partial_x^2 n_0}{2n_0}\left(\frac{\partial_x^2 n_{0m}}{\partial_x^2 n_0} - \frac{n_{0m}}{n_0}\right) + \omega_m \int^x \frac{j_{0m}(x')}{n_0(x')}dx' + \int \frac{n_{0m}(x')}{\sqrt{(x-x')^2+1}}dx'\right]. \quad (10)$$

(Note that the c_m are pure imaginary, and the correlation potential is indeed purely real.)

Plotting these terms for the δ-kicked soft-Coulomb well, where $c_m = 2ikd_{0m}$, there is no step seen; as one moves out to larger x the terms can grow very large, but there is no step structure. Figure 8 plots the response correlation potential arising from the lowest three dipole-accessible states (which are the first, third, and fifth excitations) in the sum of Eq. (10); the contributions from higher-order terms decrease rapidly, due to the decreasing oscillator strength. Moreover, carrying out the expansion to second order in k there is also no evidence of step-like structure. This is consistent with the results of the previous section; the regions where there is a step are in fact where such an expansion does not hold, and the response of the system is fully nonlinear.

The results so far show that the dynamical step feature does not appear in linear response. That is, the lack of the nonadiabatic step feature in approximations does not affect the success of the approximations in predicting linear response, because this feature only appears in situations where the system response is nonlinear. This conclusion has been based on the model 1D He atom, and we expect it to go through for the general three-dimensional (3D) N-electron case. A question might arise about systems that have states of multiple-excitation character in their linear response spectra: it is known that for TDDFT to capture such states the xc kernel must have a frequency dependence [12], indicating the underlying linear response xc potential has an essentially nonadiabatic character. For the He atom (1D or 3D), such states, however, lie in the continuum and, although they can be accessed by the δ-kick perturbation [21], they contribute much less to the spectrum than the bound states and are outside the range of frequencies for which our dynamical simulations can be trusted. A better model to explore states of multiple-excitation character is a 1D model of a quantum dot: the Hooke's atom, where two soft-Coulomb interacting fermions live in a harmonic potential. The lowest singlet excitation is predominantly a single excitation (excitation of the electronic center-of-mass coordinate), but the second and third excitations are (largely) mixtures of one single excitation and one double excitation [12,24]; one is the second excitation in the center-of-mass coordinate while the other is an excitation in the electronic relative coordinate. A dipole perturbation applied to such a system can only couple to the lowest excitation in linear response; a result that can be interpreted in terms of the harmonic potential theorem [25]. A quadratic kick, however, does excite the second and third excitations, and this is what we will consider now. We take

$$V(x,t) = \sum_{i=1}^{2} \frac{1}{2}[1 + k\delta(t)]x_i^2 \quad (11)$$

so that in Eq. (6), $c_m = ik\langle\Psi_0|\hat{x}^2|\Psi_m\rangle$.

In Fig. 9, we plot the contribution to the first-order correlation potential of Eq. (10) of the two states of double-excitation character mentioned above. Once again, there is no step structure evident. The nonadiabaticity required to capture states of double excitation in linear response is unrelated to the nonadiabatic step feature uncovered in Ref. [10].

IV. SUMMARY

In this work, we studied the correlation potential of model two-electron systems in the linear response regime to investigate the role of the dynamical step feature found in recent studies of time dynamics [10,11]. We applied a weak field to the soft-Coulomb helium atom for which we could extract the exact correlation potential. We found that step features in $v_{\rm C}$ only appear in regions far from the system, in the tails of the density, where the response of the system is in fact nonlinear. These regions, by definition, do not contribute to the measured linear response of observables. These results therefore explicitly justify the expectation expressed in Ref. [10] that the nonadiabatic nonlocal step feature that was generically found there in the time-dependent correlation potential is a feature of nonlinear dynamics and is related to having appreciable population in excited states.

This explains why adiabatic approximations can usefully predict linear response spectra in general, while these same

approximations may, in many cases, give incorrect time dynamics in the nonperturbative regime [7–11,23]. The incorrect dynamics observed in the nonlinear regime was due in part to the nonadiabatic nonlocal dynamical step found recently in these works, while the results here show that these are absent in the linear response regime. It should also be noted that TDDFT within the adiabatic approximation is still useful in many strong-field applications, as shown, for example, in Refs. [30–32]; the size of the error may be small depending on what observable is of interest. States of multiple-excitation character require a nonadiabatic approximation, but our analysis of the Hooke's quantum dot model here has shown that this is unrelated to the appearance of the dynamical step: even in dynamics where double excitations appear, the step still is absent in the linear response region.

ACKNOWLEDGMENTS

We thank Johanna Fuks for helpful comments on the manuscript. We gratefully acknowledge financial support from the National Science Foundation CHE-1152784 (for K. L.), Department of Energy, Office of Basic Energy Sciences, Division of Chemical Sciences, Geosciences and Biosciences under Award DE-SC0008623 (N. T. M.), the European Communities FP7 through the CRONOS project Grant No. 280879 (P. E.), and a grant of computer time from the CUNY High Performance Computing Center under NSF Grants No. CNS-0855217 and No. CNS-0958379.

[1] E. Runge and E. K. U. Gross, Phys. Rev. Lett. **52**, 997 (1984).
[2] *Fundamentals of Time-Dependent Density Functional Theory*, (Lecture Notes in Physics 837), edited by M. A. L. Marques, N. T. Maitra, F. Nogueira, E. K. U. Gross, and A. Rubio, (Springer-Verlag, Berlin, Heidelberg, 2012), and references therein.
[3] C. A. Ullrich, *Time-Dependent Density-Functional Theory: Concepts and Applications* (Oxford University Press, USA, 2012).
[4] M. E. Casida and M. Huix-Rotllant, Annu. Rev. Phys. Chem. **63**, 287 (2012).
[5] G. Vignale, C. A. Ullrich, and S. Conti, Phys. Rev. Lett. **79**, 4878 (1997).
[6] I. V. Tokatly, Phys. Rev. B **75**, 125105 (2007).
[7] S. Pittalis, G. Vignale, and I. V. Tokatly, Phys. Rev. B **84**, 245118 (2011).
[8] D. Hofmann, T. Körzdörfer, and S. Kümmel, Phys. Rev. Lett. **108**, 146401 (2012).
[9] J. D. Ramsden and R. W. Godby, Phys. Rev. Lett. **109**, 036402 (2012).
[10] P. Elliott, J. I. Fuks, A. Rubio, and N. T. Maitra, Phys. Rev. Lett. **109**, 266404 (2012).
[11] J. I. Fuks, P. Elliott, A. Rubio, and N. T. Maitra, J. Phys. Chem. Lett. **4**, 735 (2013).
[12] N. T. Maitra, F. Zhang, R. Cave, and K. Burke, J. Chem. Phys. **120**, 5932 (2004).
[13] D. Tozer and N. Handy, Phys. Chem. Chem. Phys. **2**, 2117 (2000); M. E. Casida, J. Chem. Phys. **122**, 054111 (2005); P. Romaniello *et al.*, *ibid.* **130**, 044108 (2009); O. Gritsenko and E. J. Baerends, Phys. Chem. Chem. Phys. **11**, 4640 (2009); M. Huix-Rotllant and M. E. Casida, arXiv:1008.1478.
[14] J. Javanainen, J. H. Eberly, and Q. Su, Phys. Rev. A. **38**, 3430 (1988).
[15] D. M. Villeneuve, M. Yu. Ivanov, P. B. Corkum, Phys. Rev. A. **54**, 736 (1996).
[16] A. D. Bandrauk and N. H. Shon, Phys. Rev. A. **66**, 031401 (2002).
[17] T. Kreibich, M. Lein, V. Engel, and E. K. U. Gross, Phys. Rev. Lett. **87**, 103901 (2001).
[18] D. G. Lappas and R. van Leeuwen, J. Phys. B **31**, L249 (1998).
[19] F. Wilken and D. Bauer, Phys. Rev. Lett. **97**, 203001 (2006).
[20] M. Thiele, E. K. U. Gross, and S. Kümmel, Phys. Rev. Lett. **100**, 153004 (2008).
[21] M. Thiele and S. Kümmel, Phys. Chem. Chem. Phys. **11**, 4631 (2009).
[22] D. G. Tempel, N. T. Maitra, and T. J. Martinez, J. Chem. Theory Comput. **5**, 770 (2009).
[23] J. I. Fuks, N. Helbig, I. V. Tokatly, and A. Rubio, Phys. Rev. B **84**, 075107 (2011).
[24] P. Elliott and N. T. Maitra, J. Chem. Phys. **135**, 104110 (2011).
[25] John F. Dobson, Phys. Rev. Lett. **73**, 2244 (1994)
[26] P. Hessler, N. T. Maitra, and K. Burke, J. Chem. Phys. **117**, 72 (2002).
[27] A. Castro *et al.*, Phys. Status Solidi B **243**, 2465 (2006).
[28] M. A. L. Marques, A. Castro, G. F. Bertsch, and A. Rubio, Comput. Phys. Commun. **151**, 60 (2003).
[29] K. Yabana, T. Nakatsukasa, J.-I. Iwata and G. F. Bertsch, Phys. Status Solidi B **243**, 1121 (2006).
[30] D. A. Telnov and Shih-I. Chu, Phys. Rev. A. **80**, 043412 (2009).
[31] I. Bocharova *et al.*, Phys. Rev. Lett. **107**, 063201 (2011).
[32] K. Yabana, T. Sugiyama, Y. Shinohara, T. Otobe, and G. F. Bertsch, Phys. Rev. B **85**, 045134 (2012).